DEUTSCHES ELEKTRONEN–SYNCHROTRON

DESY-PRC 00/04
October 2000

HERA – B

Report on Status and Prospects October 2000

Executive Summary

The HERA – B Collaboration

Contents

1 Executive Summary

1.1 Introduction

HERA – B was approved in February, 1995 to carry out a study of the physics of B meson production and decay. According the Design Report, "HERA – B is an experiment designed primarily to search for CP violation in decays of B mesons into the "gold plated" decay mode $B^0 \to J/\psi\ K^0_S$".

The ambitious schedule, calling for completion of the detector by the beginning of 1998, was not to be met. The proposed technologies for the main tracker were proven to fail quickly when confronted with the high radiation environment required for HERA – B operation. Vigorous R&D programs for both the inner and outer trackers were launched and eventually solutions were found. The detector was finally completed [1] only in February, 2000 – a two year delay.

The schedule established to build and commission the sophisticated First Level Trigger system of HERA – B also proved to be seriously over-optimistic. Production finished in 1999 and installation was largely completed by January 2000. System-level commissioning began in 1999 and continued through to the end of this year's run in late August. The trigger system is now able to find tracks starting from pretrigger seeds and map them through the tracker stations behind the magnet, as designed, but is not yet fully commissioned. There is, however, good reason to hope that the remaining problems can be solved during the present shutdown.

In the meantime, the new e^+e^-machines at KEK and SLAC have held to their (also ambitious) schedules and the associated detectors, BELLE and BABAR have reported first physics results this summer, including preliminary measurements of CP violation in the $B^0 \to J/\psi\ K^0_S$ decay mode: our primary goal according to the Design Report.

It is therefore necessary to ask if HERA – B can be reasonably expected to contribute in a meaningful way to the physics topics for which it was designed and if it is possible to use what is arguably the most sophisticated fixed-target multiparticle spectrometer and trigger system ever built for other, perhaps more mundane, physics topics. To answer these questions we must first summarize the state of the detector and estimate the efficiencies and sensitivities we can hope to achieve. Next, a survey of potential physics topics and HERA – B's competitiveness must be estimated.

The collaboration has produced a lengthy report ($\approx$ 300 pages) which attempts the answer to these questions on a rather short time scale, particularly given that the primary goal during most of this period had to be to make best of the available beam-time before the start of the long HERA upgrade shutdown. We apologize in advance for any omissions, inconsistencies and rough edges still present in the report.

This summary will first review the status of the detector and triggering systems, with emphasis on problem areas. We will then give a brief description of the data taken during the year 2000 run and finally summarize the studies of potential physics topics.

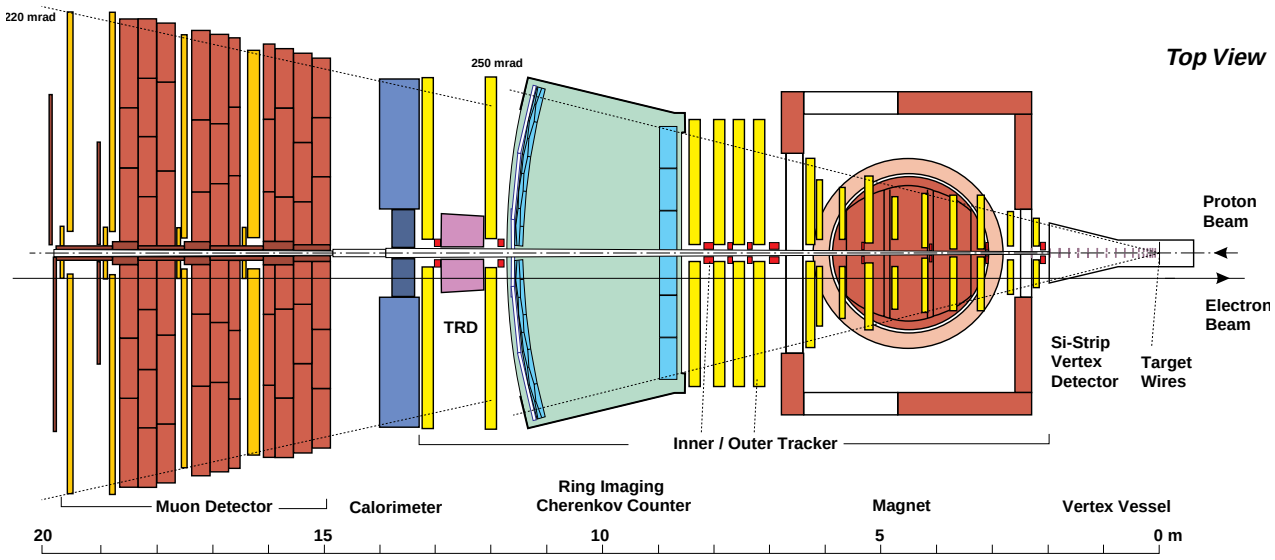

Figure 1: *The HERA – B spectrometer*

1.2 Detector Status and Plans

1.2.1 Introduction

The HERA – B spectrometer is shown in Fig. 1. We start with a very brief summary of the subsystems. Those systems in need of a more detailed status report are deferred to the following sections.

- **Target and beam:** The target has been operating regularly already since 1997. In 2000, the target was in operation during 94% of HERA luminosity periods, usually at rates between 5 and 10 MHz. Beam conditions were for the most part acceptable. Remaining problems include a large contribution to the interaction rate from unbunched beam when operating with outer and above wires and rate instability at high interaction rates. Both of these problems are being addressed together with the machine group.

- **Vertex Detector System:** The vertex detector installation was largely completed in December, 1999 (and fully completed in March 2000 with the installation of the remaining 8 modules outside the vacuum vessel). The detectors were positioned close to the beam for the majority of luminosity time during the 2000 run. The performance is as designed with signal/noise ratios of 15 – 25 (p-side, n-side), overall efficiencies >97%. Secondary vertex resolution is about a factor of two worse than expected (630 μm vs. 300 μm). This discrepancy is under study.

- **Inner Tracker:** See Section 1.2.2.

- **Outer Tracker:** See Section 1.2.3.

- **High-Pt system:** See Section 1.2.4.

- **RICH:** Installation of the RICH was completed in Spring, 1998. Since then, the system has been in stable operation. Studies show that the RICH has fully reached design specifications.

[1] With the exception of the "High-pt" system, two inner tracker stations and the TRD.

- **Transition Radiation Detector:** The TRD was installed in summer 1999 but has yet to be equipped with more than a few channels of readout electronics for budgetary reasons. The detector was powered to full high-voltage for most of the running period and operated stably. We plan to complete the installation and commissioning of this device in 2001.
- **Electromagnetic Calorimeter:** The calorimeter installation was completed in the Winter shutdown of 1997/1998. Production and installation of readout electronics lagged behind due to problems in the production and testing. By the end of the run, inner and middle regions had been equipped and the installation of electronics for the outer region had begun. The system is now complete. Energy and spatial resolutions are close to design values.
- **Muon Detector:** See Section 1.2.5.
- **First Level Trigger:** See Section 1.3.
- **DAQ and Second Level Trigger:** The hardware and software of the DAQ and the SLT are intimately intertwined since both systems use the second level buffer system, the switch and the second level processing nodes. These systems are fully installed and operating stably. A major activity of the DAQ group was growing the system as channels were added and digging out subtle bugs exposed by this growth. The DAQ/SLT system has been shown to be capable of stable operation for periods of many hours at input event rates up to 22 kHz. The second level trigger algorithm was used as a stand-in for the incomplete First Level Trigger. By the end of the run, the algorithm was close to that envisaged in the design. Suppressions and timing depend sensitively on input.
- **Fourth Level:** The 4th level hardware is complete. The farm was used for event reconstruction in the latter part of run 2000. The reconstruction time depends sensitively on interaction rate and trigger conditions. For triggered runs at 5 MHz, an average time of 4s/event was achieved. The data rates from the second level and to the computer center exceed design specifications.

1.2.2 Inner Tracker

The inner tracking system provides coverage in the area around the beam pipe up to distances of 25 cm. It provides tracking at small radii, for about 40% of all tracks from B-decays and provides input for the First Level Trigger. The Inner Tracker uses a total of 184 MSGC/GEM detectors, each with 768 anode strips organized into 10 tracking stations.

All but two (the furthest downstream) of the stations were installed and commissioned in the course of run 2000. Because of problems with the trigger outputs which precluded use in the First Level Trigger and because they are of little use for pattern recognition, the final two were not installed.

In general, the chambers and ancillary systems have run for several months and worked well, apart from some problems with the low voltage power supplies which we are investigating, together with the manufacturer. During operation, a few problems appeared which affected $\approx 2\%$ of installed chambers. All broken detectors will be repaired or replaced during the shutdown. At this point, remaining problems will be limited to defective anodes at the level of 1%.

The efficiencies of the chambers in the first inner tracking station (MS01) were determined using vertex detector tracks. The results for 7 detectors are shown in Fig. 2 as a function of GEM voltage. After individual adjustment of GEM voltages, efficiencies in the range .91 – .98 were achieved. We have recently learned that the gain variations between GEM foils (leading to the spread in efficiencies)

is most likely due to a mismatch between electrodes on the two sides of the foil. An efficiency study for the entire system awaits tuning of the alignment and general track-finding code.

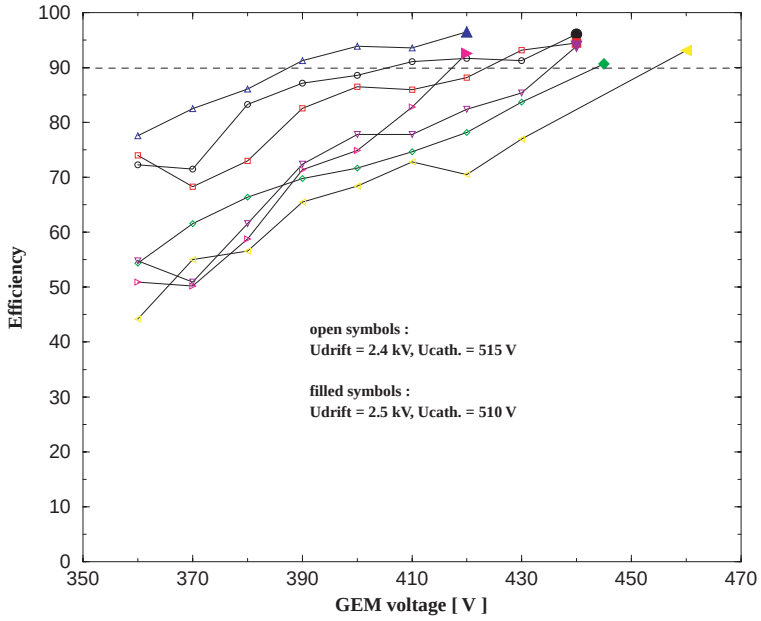

Figure 2: *Efficiency of 7 detectors of station MS01 versus GEM voltage for fixed cathode and drift voltages. The filled symbols show the efficiencies for the current voltage settings after individual gain adjustments.*

Four of the tracking stations behind the magnet will have to provide hit information for the First Level Trigger. To guarantee high efficiency, each of these stations has two layers per view whose trigger outputs are ORed in the front-end electronics. Hit information comes from discriminating the analog signal for each strip and subsequent ORing of 4 neighbors. Each readout chip delivers 32 hit/no-hit signals for each event.

The present trigger installation cycles correctly but, because the discriminator threshold had to be raised to prevent oscillation, it does not give adequate efficiency. By reducing the voltage swing of the trigger output drivers and reworking the grounding scheme, the oscillation could be overcome. Three double trigger layers were installed and operated in August. The measured efficiency is at least 90% and compatible with 100%.

During the shutdown, all detectors will be taken out of the experiment. Broken ones will be repaired or replaced. All front end cards for trigger layers will receive a new version of the readout chip to correct an error with the analog pipeline length. New trigger driver boards will be installed and the path to the First Level Trigger will be commissioned during the shutdown. By the end of the shutdown, the system will be fully installed, including the remaining two trigger stations.

1.2.3 Outer Tracker

The Outer Tracker provides coverage starting from about 25 cm from the beam pipe up to the full aperture of the spectrometer (220 $\times$ 160 mrad). The Outer Tracker is organized into 13 super-layers extending from the vertex vessel to the calorimeter. Each super-layer is logically segmented into 12 sectors of varying dimensions. The Outer Tracker is built from honey-comb drift cells with a wire

pitch of either 5 mm or 10 mm, depending on sector. Four of the super-layers behind the magnet are used in the First Level Trigger. The trigger layers are doubled for high efficiency.

The installation of the Outer Tracker was completed in January 2000. Since then, the system has been available >90% of the time. The high voltage and gas systems are operational and fully integrated with the global HERA – B slow control.

Apart from a potentially serious problem with high voltage stability (described below), only relatively minor and solvable problems were encountered:

- On two occasions, the system was out of operation due to leaks in the gas system. Finding the leaks proved to be a difficult and time consuming operation, resulting in a total downtime of about two weeks. The failure modes have been identified: dirt in bellows of pumps and loosening of gas fittings and measures have been taken to eliminate them.
- 138 (of 7200) readout boards were not giving signals. Most of these failures probably occurred at assembly (cables coming loose). Improvements in assembly procedures are expected to reduce this problem to a negligible level.
- The thresholds of the four super-layers used in the First Level Trigger had to be raised because of additional noise induced by connections between the TDC boards and trigger electronics. We are studying ways to reduce or eliminate this additional noise.

From the beginning of Outer Tracker operation in July 1999, high voltage groups[2] started to fail. The average failure rate was one group per 5 hours of operation. By the end of the run, 6.9% of high voltage groups had failed.

The failure rate was particularly high in the first assembled super-layer. It was suspected that the reason for the failures was mechanical instability since the modules of this super-layer had not been reinforced with carbon fiber stiffener rods. This super-layer was removed and overhauled in December 1999, then reinstalled. Since the repair, the failure rate decreased by a factor of 10, one of the lowest rates in the system.

Several initial tests and observations indicated that discharges and mechanical module imperfections might have been responsible. After the end of the run in September 2000, inspection of damaged modules revealed a completely unexpected source of failure. Of the modules inspected, 39 of the 49 "shorts" were caused by burnt-in carbon traces of varying resistance in residue left over from the soldering process across either of two capacitors on the bottom side of the high-voltage board responsible for distribution to a 16-wire group. A total of 17 capacitors are mounted on this board, 15 on the top and 2 on the bottom. Failures were seen only in connection with the 2 capacitors mounted on the bottom. This systematic difference is most likely due to differing mounting techniques.

While it is clear that shorts across the capacitors are implicated in the vast majority of the failures, we are concerned about remaining failure modes which might by a first indication of future problems. We are currently working to understand the experimental findings and making tests to try to reproduce the failures on a test bench.

During the shutdown, all bottom-side capacitors will be exchanged using a clean soldering technique. Also all modules which have not yet already received carbon fiber stiffeners will be reinforced

[2] A high voltage group consists of 16 channels.

(mainly 2 half super-layers). All modules will be subjected to a rigorous high voltage test to identify short and hot wires, while mechanically exercising them. Improved assembly and test procedures should reduce the number of unplugged readout boards to nearly zero.

We have determined the Outer Tracker cell efficiency for data taken at various times throughout the run. As an example, Fig. 3(a) shows the efficiency of cells in one 5 mm module of one sector of one super-layer, near the end of the run. From the fitted curve, the efficiency in the plateau was determined to be 0.93. The region has a radius of about 2 mm around the wire. Outside the plateau region, (near the edges of the hexagonal cell), the efficiency drops to zero[3]. The efficiencies of the 128 cells of the same module sector are mainly above 0.90, as shown in Fig. 3(b).

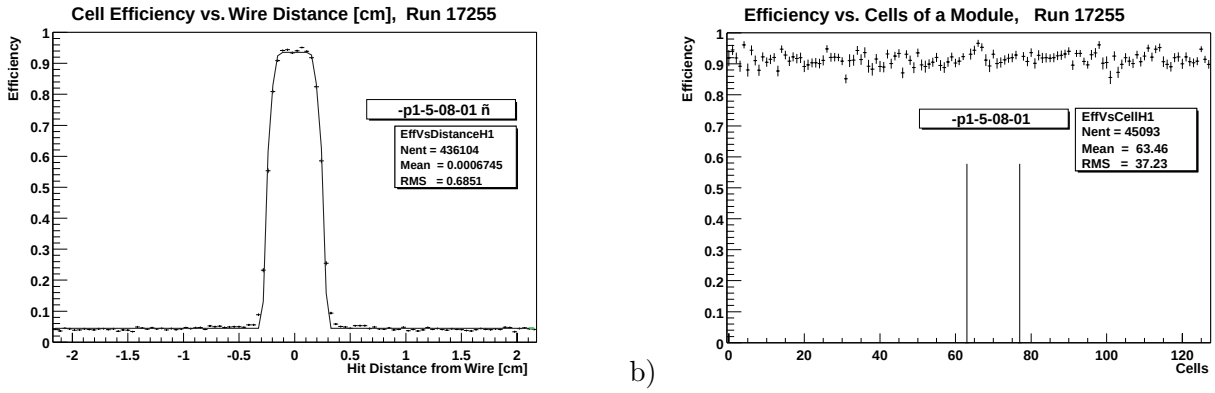

a) b)

Figure 3: *a) Dependence of the cell efficiency on the distance from the anode wire (5 mm cell) for module 8 in sector 1 in stereo layer 5 of super-layer PC1–. b) Efficiency of the 128 cells of the same module.*

The results of the same analysis applied to 8 super-layer halves in the main tracker behind the magnet for two runs are shown in Fig. 4, as a function of the discriminator threshold setting averaged over the super-layer half. A clear threshold dependence is seen. The runs 17255 and 17254 were taken nearby in time and differ only in high voltage settings and therefore gain. Most of the data taken during year 2000 run was taken with settings similar to those of run 17255 because of the high-voltage stability problem described above. It now seems likely that we will be able to run with the increased gain settings of run 17254 and thus benefit from the increased efficiency.

Two methods were used to check the resolution of the chambers. One method estimated a "local" resolution by comparing the hit positions of hits on adjacent double layers. The method has the advantage of being insensitive to alignment effects and extrapolation errors. A resolution of 240 μm – 300 μm was found, compared to a value of 500 μm – 700 μm, estimated using found tracks. The discrepancy is most likely due to our still preliminary alignment.

1.2.4 High-p_T Chambers

The concept of the high-p_T trigger is as follows: tracking chambers with a pad-type readout are placed within the spectrometer magnet. Pad hits are input to dedicated processors, and high-p_T tracks are selected based on the hit patterns. Such tracks tend to bend little or make larger angles with respect to the beam, and their hit-patterns are distinct from those caused by minimum bias tracks.

[3]By construction, the neighboring cell overlaps sufficiently to ensure negligible efficiency drop in the edge region.

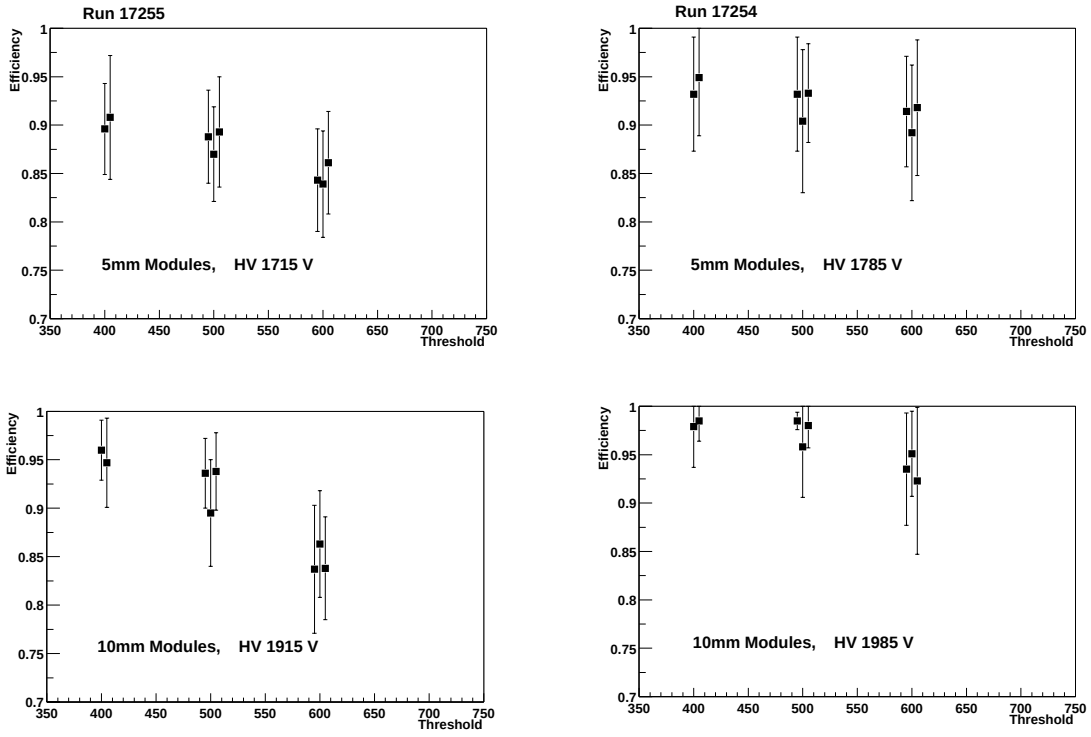

Figure 4: *Average efficiency of the PC super-layer halves for runs 17255 and 17254 taken under identical conditions, except the high voltage. The corresponding gains are 1.17 and 1.46. The horizontal axis is the preamplifier threshold voltage in millivolts.*

The tracking chambers with pad readout come in two types: gas-pixel chambers for the region nearest the beam, and straw-tube chambers with "pickup-pads" for the larger outer region.

The gas-pixel chambers use short anode wires oriented parallel to the beam. The tracks going from the main vertex to the inner high-p_T chambers are almost parallel to the wires resulting in large primary ionization and sharp rise times.

The straw tube chambers utilize straw tubes against which are positioned printed circuits consisting of a pad pattern. These pads are positioned very close to, or in contact with, the outer surface of the straw tubes. A gas avalanche occurring at an anode wire then induces an image charge on the pad directly above the avalanche.

There are a total of 12 chamber halves organized into 3 super-layers: six gas-pixel chambers for the inner region and six straw tube chambers for the outer region.

Status of Inner Chambers: All inner chambers were installed during the 2000 running period and were operational at a voltage setting at least 50 V above the value corresponding to the beginning of the efficiency plateau. During the last month of data taking, the chambers were operated routinely along with the rest of the HERA – B detector. The number of dead channels is relatively small: out of 11 960 channels, 18 are dead due to missing wires or disconnected cables and 12 have lost one wire (of two in the cell) resulting in an efficiency loss of about 30%.

The single-cell efficiency was determined using tracks defined by matching VDS, ECAL, and RICH segments and two of the three high-p_T stations (e.g., PT1 and PT3). All known dead and hot

channels were excluded. The efficiencies obtained for different chambers and cell sizes are shown in Fig. 5.

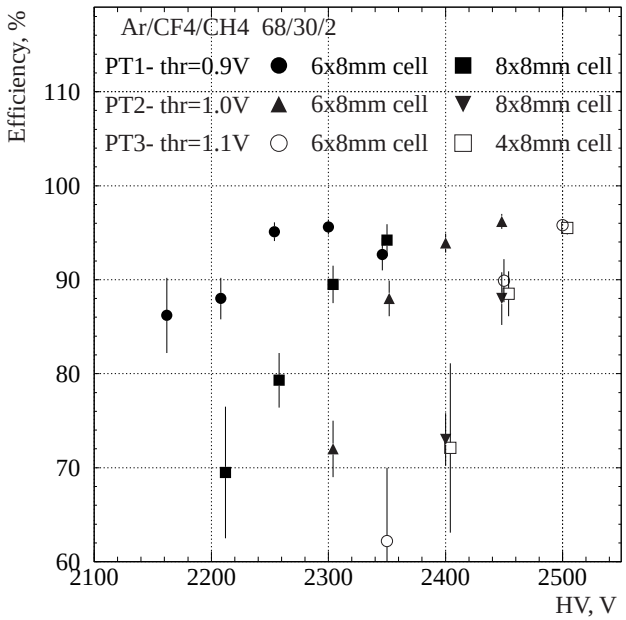

Figure 5: *Efficiencies measured for inner high-p_T chambers during the 2000 run using VDS-ECAL-RICH tracks.*

The efficiency measured reaches a plateau of about 96% and does not increase further. This could indicate that some fraction of the reference tracks are ghosts; alternatively, there may exist a timing problem or an electronics inefficiency with large signals. Previous tests at the ITEP synchrotron yielded a single-cell efficiency higher than 99% for fluxes up to about 5×10^5 particles/cm^2-s. These measurements, however, were performed without a magnetic field.

Status of Outer Chambers: During the 2000 running period, four of six outer high-p_T chambers were installed and run regularly at nominal high voltage. All but two of 1488 straw tubes were active. The very limited access to the detector precluded installation of the remaining two chambers, they will be installed during the present shutdown.

The installed chambers were partially instrumented with front-end cards and read out. Substantial intermittent noise and oscillations were seen on the front-end ASD-8 cards which prevented us from measuring chamber efficiencies or inputting meaningful signals to the pretrigger electronics. During the present shutdown, we will attempt to trace the sources and eliminate the oscillations.

1.2.5 Muon

The muon system provides a pretrigger signal for the First Level Trigger and is used for muon identification in the offline analysis. It consists of a muon filter and four super-layers of muon chambers. Each super-layer has pixel chambers covering the area near the beam pipe. The outer regions are covered by a combination of tube and pad chambers. The outer regions of the first two super-layers consist of three layers of muon tube chambers with 0^o and $\pm 20^o$ views. The outer

regions of the third and fourth super-layers consist of one 0^o layer with both anode and pad readout. The pads (and pixels) of these layers are used in the muon pretrigger. The First Level Trigger also relies on the tube chambers of the first, third and fourth layers for tracking.

All 342 tube chambers, 132 pad chambers and 16 pixel chambers are installed and running. Chamber operation has been smooth and reliable.

The major cause for concern in the muon system is the efficiency of the pad chambers. The measured efficiencies for the MU3 and MU4 pads are 75% and 68% respectively. Since one pad from each chamber is required in the muon pretrigger, the efficiency per track is just 51% and since most triggers require two tracks, the pretrigger efficiency is just 26%. Studies are underway to understand how to improve on this. Foreseen improvements including a better grounding scheme, installation of additional filter capacitors, a modified termination scheme, repair of high-voltage problems and broken readout channels, and operation at higher chamber bias (high voltage) are expected to improve the efficiency to ≈90%, resulting in an overall 2-track pretrigger efficiency of 66%. Improvements beyond this will almost certainly require replacement of the front-end amplifier board (ASD-8). The ASD-8 amplifier has a shaping time of 6 ns which is a poor match to the 25 ns rise time of the pad pulses. We are looking into the feasibility of designing, producing and installing new amplifier cards in the present shutdown.

The efficiency of the tube chambers is also somewhat uncertain. A tube efficiency of $> 99\%$ was measured in a test beam, however a measurement in situ shows efficiencies in a range from 96.6% – 98.3%, depending on super-layer, despite the fact that we are running the chambers well above the knee of the plateau curve. The discrepancy between the test beam result and the in situ measurement has not been fully tracked down however it is due in part to some residual broken channels ($\approx 1\%$) which we expect to repair during the shutdown. We also suspect that the sample of reference tracks includes some ghosts.

1.3 Trigger Status and Plans

We first briefly review the status of the pretrigger systems and the First Level Trigger. An extended discussion of the trigger efficiency of the pretrigger/FLT system follows.

1.3.1 Calorimeter Pretrigger

The calorimeter pretrigger system has been in operation since the beginning of the 1999 run, providing a high-E_T trigger which allowed detection of the J/ψ in its e^+e^-decay mode. During the course of the 1999, 2000 runs, the system grew and was finally completed near the end of run 2000. By Summer 2000, the majority of the system ($\approx 80\%$ by end July) was fully integrated with the DAQ and running reliably. The intrinsic efficiency of the system was determined by comparing clusters found in the offline analysis with those generated by the pretrigger system and inserted into the event stream via the FLT electronics. The average efficiency for working cells is 95%.

1.3.2 Muon Pretrigger

The muon pretrigger has been in operation and supplying pretriggers since July of this year. Coverage of the muon pad chambers is complete. The efficiency of the system was measured using a technique similar to that used to measure calorimeter pretrigger efficiency. Half of the system was found to

have an efficiency >99% while 28% showed efficiencies between 95% and 99% and 7% have efficiencies between 80% and 95%. The remaining channels suffered from hardware failures in the readout chain. A major reason for the inefficiencies has been traced to bit errors in the pretrigger messages. The errors most likely occur in a single FLT module in the transmission chain. (If this turns out to be the case, this module will be repaired or replaced.) The electronics needed to cover the pixel chambers exists and has been tested. The installation will be completed during the shutdown.

1.3.3 High-Pt Pretrigger

A small test setup consisting of six link boards and four pretrigger boards was installed in the experiment and, after considerable effort to tune the optical links, worked essentially error-free during periods without target operation. During data taking, bit errors occurred occasionally, presumably due to the larger number of hits in the data streams. This may imply that the DC offset for the optical receivers should be increased at higher interaction rates. The problem is under study (see Sect 1.3.4.

Using data from the inner chambers collected during minimum bias runs at various interaction rates, we have estimated the pretrigger rate. This rate as a function of interaction rate is shown in Fig. 6 (for inner chambers only). All channels with occupancy larger than 20% have been masked out. The average number of pretriggers is 0.18/BX at an interaction rate of 5 MHz, about 60% larger than the Monte Carlo prediction of 0.11/BX. The contributions from the $+x$ and $-x$ sides are equal. The pretrigger rate drops if one makes more stringent cuts on noisy channels. The pretrigger rate is 1.06/BX at an interaction rate of 20 MHz, again somewhat larger than the Monte Carlo prediction of 0.61/BX. The rate of the high-p_T pretriggers in coincidence with the electron (FLT-SLT trigger with $p_t > 1.5\,(1.0)$ GeV/c is 0.82/BX at 2 MHz. This is a factor of two larger than the Monte Carlo prediction.

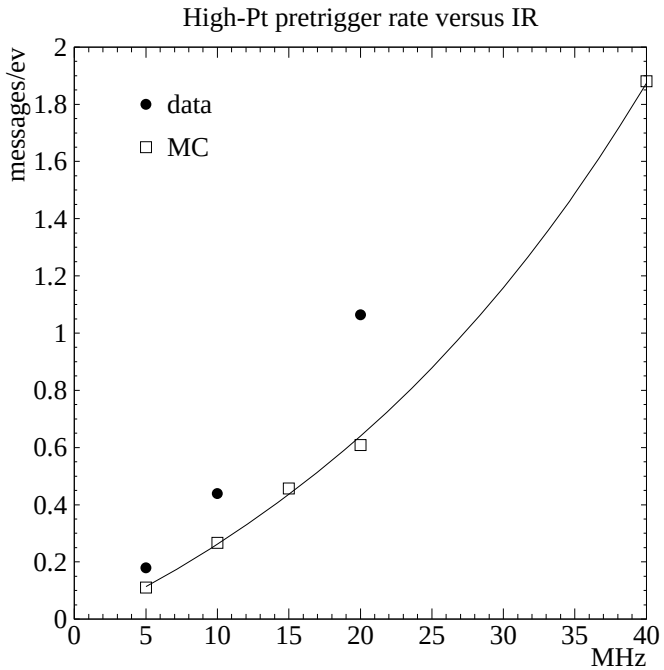

Figure 6: *High-p_T system pretrigger rate as a function of interaction rate.*

1.3.4 Optical Links

Optical links are used for transmitting hit data from the trackers to the pretrigger systems and the TFUs. A serious concern is whether the present optical links can provide the required stability over an extended period of time. In the present scheme, offset and modulation currents are adjusted with potentiometers. Because of different attenuation for the different optical fibers, temperature drifts and other effects, the pre-adjusted values have often proven to be outside the dynamic range of the receiver. The potentiometers are not accessible once the boards are installed. Hence any adjustment requires removal of the board which is a delicate and lengthy procedure. Thus we are considering adding the capability to adjust the offset and bias currents remotely. A new optical transmitter piggy-back is being designed and the feasibility of producing and replacing some or all of the links installed in the experiment is being evaluated.

1.3.5 First Level Trigger

The FLT attempts to find tracks in the tracking super-layers behind the magnet starting from seeds defined by the pretrigger systems (4 main-tracker super-layers and, for the muons, also 3 muon super-layers). It is capable of making cuts on kinematical properties of tracks, of requiring any number of tracks from combinations of pretrigger sources and of combining tracks pair-wise, and imposing cuts on the pair mass.

The track finding is done in an array of 82 interconnected purpose-built processors (called Track Finding Units). Each processor takes input from one section of one super-layer. Messages containing track parameters pass from pretrigger systems to TFUs and then from TFU to TFU and finally (for accepted tracks) into Track Parameter Units which calculate and cut on kinematical parameters, passing on accepted tracks to the Trigger Decision Unit which is responsible for the final trigger decision.

By the beginning of 2000, the FLT electronics had been largely installed and was undergoing system tests. Many problems were yet to be solved, among them:

- The optical links were not working properly and had to be hand-tuned. Eventually most optical links (96%) were made to work and those with significant error rates ($> 10^{-6}$) were set "on" meaning that all channels serviced by that link showed hits for all events.
- Other system level hardware problems had to be corrected to stabilize the system, such as cooling in the TFU crates and unstable "repeater boards" between TFUs.
- The Outer Tracker was not behaving at performance levels: many channels were being lost due to high voltage problems. The resulting inefficiencies were large enough to kill any hope of using the FLT as a trigger until a way had been found to mask ON the dead areas.
- The cell spacing of the Outer Tracker was found to be less uniform than expected, due to the modular construction. A new software tool had to be written to minimize the resulting inefficiencies.
- Links between pretriggers and the track-finding units were flaky and had to be stabilized.
- Many of the tools needed to control, monitor and simulate the FLT were found to be either missing or inadequate and had to be either written or rewritten.

Nonetheless, by the end of the run, the system was working at the level of finding tracks with fair efficiency (see below) and producing messages containing lists of triggered tracks and their coordinates for the second level trigger. The FLT was also used as a trigger in the last days of the run, with mixed success. This is further discussed in the next section.

1.3.6 Trigger Efficiency Estimates

In the remainder of Section 1.3, we go into quite some detail to explain our present understanding of the trigger efficiency of the complete triggering chain based on data taken during the year 2000 run and our expectations for startup in 2001. Readers not interested in the details are invited to skip to tables 2 and 4.

1.3.7 FLT Track Finding Efficiency Estimate (OTR)

Table 1: *Efficiency factors needed to calculate the track finding efficiency of the First Level Trigger. Row 13 is the calculated efficiency based on the given figures. The upper limit of the range given in the last line under "present" has been increased to accommodate a measurement not consistent with the model of 74% (see text).*

		Efficiency model	
		Present	**Potential**
1	Working-cell efficiency	0.90	0.95
2	Dead single cells	0.08	0.015
3	Dead double cells	0.08	0
4	Masking efficiency	0.8	1
5	Partially working optical links	0.04	0
6	Efficiency TDC-TLB links	1.00	1
7	Efficiency optical links TLB-TFU	1.00	1
8	Hit efficiency	0.968	0.997
9	All trigger layers hit, 1 track	0.68	0.96
10	Lookup table coding problems	0.97	>0.97
11	Understood geometrical effects	0.95	>0.95
12	Other geometrical effects	0.92	>0.92
13	Tracking efficiency (model)	0.58	>0.81
14	Adjusted track efficiency	0.58 - 0.74	0.81 - 0.96

In this subsection we summarize our present understanding of the FLT tracking efficiency in the four Outer Tracker super-layers. There are several ways to arrive at efficiency estimates using data sets taken under different conditions, using simulation and paper models based on known efficiencies. We find inconsistencies when comparing the various estimates which we are working to resolve.

We start with a paper model. The input numbers are given in the column labeled "Present" of Table 1. Row 1 of this table is the measured single-cell plateau efficiency (see the Outer Tracker section). Most dead single cells (row 2) are due to disconnected high voltage groups. Dead double cells (row 3) are mainly due to malfunctions of ASD8 preamplifier cards or misplugged cables from chamber to preamplifers.

As described in the paragraph entitled "Optical link performance tests" of the FLT report, a comparison was made of occupancy distributions as seen in the wire memory of the TFUs and in the offline analysis. Discrepancies at the level of 1.5% are seen. Most of these errors can be attributed to failures in the masking technique. If we assume that the entire 1.5% is due to such failures, the fraction of successfully masked channels must be 0.8 (row 4) since the total number of dead double layers is 8.0%.

At run startup, the optical links connecting the detector to the TFUs are checked and if a significant bit error rate is found ($> 10^{-6}$), the corresponding cells are switched on (i.e. the TFU sees a hit for each cell). Typically, 4% of the links were switched on (row 5). Since they were on, no inefficiency is incurred (we list them in the table for completeness). The remainder of the links were 100% effective (rows 6,7).

To first order, the hit efficiency is:

$$P_{hit} = P_3 \cdot P_4 + (1 - P_3) \cdot (P_2 \cdot P_1 + (1 - P_2) \cdot P_1 \cdot (2 - P_1))$$

The numbers refer to the rows in Table 1. Plugging those numbers into the formula yields a hit efficiency of 96.8%. Thus the probability that all hits needed to find a track are present is $P_{hit}^{12} = 68\%$, since 12 hits are required.

Next, we turn to the results of a simulation. The simulator does a "bit-wise" identical emulation of the FLT hardware and can take input from either Monte Carlo or data, in this case we use Monte Carlo. The Monte Carlo takes into account the Outer Tracker single-cell efficiency as well as the complete map of dead and hot channels. The simulator also uses the dead/hot channel map to turn on dead channels but assumes 100% masking efficiency in place of the 80% given in the table. The simulator result of 80% for percentage of tracks with all hits becomes 67% after a global correction for the non-masked (1.5%) channels is applied, in good agreement with row 9.

The next factor to consider is the track-finding efficiency of the FLT itself, given that the hits are present. The simulator shows a total drop in efficiency of 15% from "algorithmic" effects. We separate these effects into 3 factors in the table:

- Lookup table coding problems: The algorithm used to generate the lookup tables uses an oversimplified geometrical model of the detector. Most of this inefficiency can be recovered with a more realistic model.
- Understood geometrical effects: These are mainly due to irregularities in the cell spacing of the Outer Tracker arising from its modular structure. It is in principle possible to recover most of this ineffeciency by treating the position of each wire individually when generating the lookup tables.
- Other geometrical effects: These effects are not yet understood.

When these effects are taken into account, an overall tracking efficiency of 58% is found. This can be compared with measured values derived from other studies:

- Data was taken while triggering on the calorimeter. The FLT was in "transparent" mode, i.e. found tracks were recorded but the FLT decision did not actually produce triggers. Reference tracks were defined using reconstructed ECAL-RICH-VDS matches. The reference tracks were matched to tracks in the FLT output record 74% of the time.
- Compare the same set of reference tracks with the simulator output (rather than the recorded FLT record) on an event by event basis. The measured efficiency is found to be 59%.

- Run the simulator on the sample of J/$\psi \to \mu^+\mu^-$ events accumulated over the summer. The result is 59%. (Additional inefficiencies in the muon tracking are not included in this estimate.) The estimate is clearly somewhat biased by the trigger selection which should, if anything, lead to an overestimate.

The discrepancy between these values is not understood. Until the inconsistency is resolved, we use the lowest and highest measured values to indicate the range: 58% – 74% (line 14).

We also list in Table 1 the numbers we expect to achieve by the end of the present shutdown. Improvements in the Outer Tracker's single-cell efficiency and dead channel count will result in a findable track (i.e. all hits present) efficiency of 96%. After losses in the FLT algorithm are taken into account, this will be reduced to between 81% and 96%. Finally, we adjust the lower end of the range to the lower limit of the present range multiplied by the ratio of the values given in line 9. We hope to reduce the errors on this estimate in the near future.

1.3.8 Trigger Efficiency for J/$\psi \to e^+e^-$

Table 2: *Efficiency for J/$\psi \to e^+e^-$. All rows are event level efficiencies.*

		Model		**Design**
		Present	**Potential**	
1	Geo., ktrig 500, m > 2 GeV	0.34*	0.34*	0.45
2	Missing low angle coverage	0.44*	1	1
3	ECAL pretrig eff. (incl coverage)	0.62	0.95	1
4	Tracking efficiency (2 tracks)	0.34 - 0.55	0.66 - 0.92	1
5	Frontend pipeline overflows	1	1	1
6	Total efficiency	0.032 - 0.051	0.21 - 0.30	0.45
7	Ratio to design	0.07 - 0.11	0.47 - 0.67	1
Triggered rates (5 MHz)				
8	direct J/$\psi \to e^+e^-$ / hour	1000 - 1700	7000 - 10000	15000
9	B $\to$ J/$\psi \to e + e-$ / hour	.7 - 1.2	5 - 7	10

* to be verified

In Table 2 we summarize our understanding of the geometrical and trigger efficiency for J/$\psi \to e^+e^-$ as seen near the end of Run 2000, what we expect to achieve and a comparison of these to the values given in the Design Report. Rows 1 and 2 of the table come from the FLT simulation[4]. Row 3, the pretrigger efficiency was, at the time of this estimate (end July), dominated by missing calorimeter readout and pretrigger coverage but also includes an intrinsic inefficiency of 5% when compared to the offline calorimeter reconstruction (hence the 95% in the "Potential" column). Row 4 is explained in section 1.3.7.

Row 5 gives that the efficiency factor due to the loss of triggers which arrive after the event data has left the frontend pipelines is zero. Since the trigger decision is made in the required time when the processor network is unloaded, the number can always be adjusted to 1 by adjusting the

[4]We believe these numbers to be correct, however we were unable to dispel all doubts before the deadline for publication.

interaction rate. The issue then is the maximum interaction rate imposed by congestion in the processor network. By design, the processor network is intended to cope with interaction rates up to 40 MHz. A conclusive measurement has not yet been made.

Over the lumi upgrade shutdown we expect to complete the low angle coverage by introducing the Inner Tracker into the trigger, utilize the complete calorimeter coverage, improve the Outer Tracker and work to better understand and improve the FLT efficiency. Row 7 shows that we expect the final efficiency to lie between a third and two thirds of the design value. Much of the difference between the Design Report and present estimates comes from the geometric and kinematical factors shown in row 1. The number given in the Proposal (32%) is much closer to the presently accepted value. The figure given in the Design Report is clearly over-optimistic.

Note that, as in the Design Report, we have not included SLT efficiency in this table since it is highly correlated with reconstruction efficiency. The estimates of reconstruction efficiency given throughout the document include SLT efficiency, except when specifically itemized. A discussion of the observed and simulated SLT efficiency can be found in the SLT report.

1.3.9 Trigger Efficiency for J/$\psi \rightarrow \mu^+\mu^-$

Table 3 shows factors entering into the calculation of the muon pretrigger efficiency for a single muon as well as additional factors needed to determine tracking efficiency in the muon system. The numbers in the 2nd column refer to the present setup, those in the 3rd to the setup at startup in 2001.

The pad and pixel chambers (super-layers 3 and 4) are used to define pretrigger candidates and three of the four muon tube chambers (super-layers 1,3,4) are used to define track seeds in preparation for tracking through the tracker super-layers. At present, only the pad chambers have been used in the pretrigger. The average pad efficiency is 71%, implying a coincidence efficiency of 51% (row 1). Some losses are measured in the pretrigger and peripheral electronics (row 3). The overall per-track efficiency of the pretrigger system is given in row 4.

Pretrigger candidates initiate track-finding in the FLT processors dedicated to muon tracking. The tracks are followed through 3 of the 4 muon super-layers before being passed into the main Outer Tracker processors, thus the efficiency of the muon tube chambers also affects the trigger efficiency. Since 5 tracking layers are used, the effective hit efficiency is raised to the fifth power, leading to an overall probability that all hits needed to find a track are present of between 86% and 95%. (row 10).

The factors pertaining to intrinsic FLT efficiencies (rows 11 - 13) are closely related to the corresponding factors in Table 1. See Section 1.3.7 for explanations.

The full tracking efficiency (including Outer Tracker) is obtained by multiplying the values from row 14 of Table 1 for tracking in the Outer Tracker: 39% to 56%. This can be compared to two other efficiency estimates:

- A data set was accumulated using a trigger which required a single track at the first level. The second level then looked for two tracks using the same algorithm used for the bulk of the muon-triggered running. A (somewhat biased) tracking efficiency can be derived by comparing the rate of J/ψs found in this data with that seen with the SLT-only runs taken nearby in time. The resulting efficiency is 19% per track.

Table 3: *Efficiency factors needed to calculate the muon pretrigger efficiency and track finding efficiency in the muon system. Row 15 is the calculated track-finding efficiency in the muon chambers, based on the given figures. The values given in line 16 refer to the full efficiency for finding a track in both the muon and outer tracker chambers. Line 16 has been adjusted to accommodate all of the measurements.*

		Efficiency Model	
		Present	**Potential**
1	MU3 · MU4 pad efficiency	0.51	> 0.90
2	Dead/hot channels (muon pads)	0.01	0.01
3	Pretrigger system efficiency	0.92	1
4	Overall pretrigger efficiency/trk	0.46	0.90 - 0.98
5	Tube efficiency (working cells)	0.85 - 0.90	0.85 - 0.90
6	Double layer tube efficiency	0.97 - 0.99	0.97 - 0.99
7	Dead/hot muon tubes (single layer)	0.06	0.02
8	Link efficiency	1.00	1
9	Effective hit efficiency	0.97 - 0.99	0.97 - 0.99
10	Hits in all tube chambers/trk	0.86 - 0.95	0.86 - 0.95
11	Lookup table coding problems	0.94	>0.94
12	Understood geometrical effects	0.95	>0.95
13	Other geometrical effects	0.89	>0.89
14	Muon system tracking	0.68 - 0.76	0.68 - 0.95
15	Complete Muon + OTR tracking	0.39 - 0.56	0.55 - 0.91
16	Adjusted complete tracking	0.19 - 0.56	0.27 - 0.91
17	Pretrigger & tracking(adjusted)	0.09 - 0.26	0.24 - 0.89

- A data set with a 2-track FLT trigger and 2-track SLT trigger was accumulated in the last days of the run. No J/ψ was seen so no efficiency can be derived. However an upper limit of 28% efficiency per track can be inferred by comparing with SLT-triggered runs taken nearby in time.

The first of these measurements is not consistent with the range given on line 15. We are therefore, once again, forced to adjust the range to accommodate this lower value (line 16). Finally, we multiply in the pretrigger efficiency given on line 4 and obtain our final estimate of pretrigger + FLT efficiency for a single track of 9% – 26% for the current setup.

The efficiency estimates for J/$\psi \rightarrow \mu^+\mu^-$ are given in Table 4. The uncertainties in both the muon tracking and the main tracker tracking lead to a large uncertainty in the total J/ψ efficiency. In the present setup, the maximum efficiency estimate is 2.7% of the design value. Foreseeable improvements should bring the efficiency up to near 79% of the design value. Most of the uncertainty lies in the "algorithmic" problems of the First Level Trigger and inconsistencies between the various efficiency measures. We are working on narrowing down the errors on these estimates with high priority.

Some losses are seen due to triggers arriving too late (row 5) even at an interaction rate of 5 MHz, implying an upper limit on the interaction rate somewhat less than 5 MHz for the present setup. Foreseen improvements will reduce these losses to at most 8% at 5 MHz interaction rate. At least part of the reason for the present high latency is congestion in the FLT network stemming from the large number of switched on channels. We expect improvements after the number of masked

Table 4: *Efficency for $J/\psi \to \mu^+\mu^-$. All rows are event level efficiencies (i.e. 2 tracks).*

		Model		Design
		Present	**Potential**	
1	Geometry, p > 5 GeV	0.62	0.62	0.62
2	Missing low angle coverage	0.44*	1	1
3	Pretrig, tracking efficiency (2 tks)	0.008 - 0.07	0.06 - 0.79	1
4	Frontend pipeline overflows	0.77 - 0.88	0.92 - 1	1
5	Total efficiency	0.002 - 0.017	0.03 - 0.49	0.62
6	Ratio to design	0.003 - 0.027	0.06 - 0.79	1
Triggered rates (5 MHz)				
7	direct $J/\psi \to \mu^+\mu^-$ / hour	70 - 560	1000 - 16000	21000
8	$B \to J/\psi \to \mu^+\mu^-$ / hour	0 - 0.4	0.7 - 12	15

* to be verified

channels is reduced to the number given in line 2 of Table 1 and the the 4% of non-working optical links are repaired. Further ways to decrease the trigger latency are under study (e.g. using 2 rather than 3 muon super-layers in the track propagation).

1.4 Run 2000

A summary of the major data sets taken since April of this year is given in Table 5. The FLT tracking was under intense development during the run and was not available for taking production data, except at the very end. We therefore triggered using calorimeter and muon pretriggers and the Second Level Trigger. The Trigger Decision Unit of the FLT received the pretrigger messages and issued a trigger if a required number (one or two) of pretrigger candidates were seen. The second level made further cuts on p_T and possibly mass then attempted to find tracks associated with the pretrigger candidates.

After a short run with a minimum bias trigger, we concentrated on developing the Di-lepton trigger. At first, we triggered with the electron pretriggers and the SLT. During this period, the SLT projected pretrigger candidates directly into the vertex detector, with no intermediate tracking in the OTR. The bulk of the data of the year 2000 sample was taken with these conditions. When the Outer Tracker stabilized and an alignment became available in mid-June, the second-level algorithm for tracking behind the magnet was commissioned. At the end of June, we introduced muon pretriggers and ran simultaneously with both electron and muon pretriggers. Finally, in the last two weeks of the run, we turned on tracking at the first level and took data with both single and double track conditions at the FLT and both single and double track requirements at the SLT. Most of the di-lepton data was taken with an interaction rate of 5 MHz. The single lepton data was taken with a 2 MHz interaction rate. Higher rate running (up to 40 Mhz) was tested on a weekly basis.

The invariant cross section per event, as derived from the minimum bias sample, is shown in Fig. 7 together with the reconstructed Monte Carlo. The Monte Carlo agrees with the data to about 20% except for the high p_T region where the measured spectra are somewhat harder. For the charge ratio shown in the bottom of the figure, most acceptance corrections cancel and, for $p_T > 0.5$ GeV/c, the data and Monte Carlo are in good agreement. The relative deficit of low-p_T positive particles in

Table 5: *The major data sets taken during the year 2000 run. The active pretriggers (E = ECAL, μ = Muon) are shown in the "pre" column. The "FLT" column distinguishes between runs with no tracking requirements and a requirement of 1 track or 2 tracks. The "SLT" column gives the SLT requirements: 1 ⇒ 1 track, 2 ⇒ 2 tracks, V ⇒ Vertex detector tracking, O ⇒ Outer tracker tracking.*

Type	Start	Stop	Trigger			Events	Time(min)	
			Pre	FLT	SLT	$\cdot 10^{-6}$	total	live
Min Bias	10 Apr	14 Apr	-	-	-	2	2000	-
Di-lepton	29 Apr	13 Jun	E	-	V,2	12	10387	7508
Di-lepton	15 Jun	27 Jun	E	-	OV,2	1	1385	953
Di-lepton	28 Jun	16 Aug	Eμ	-	OV,2	3.7	9363	4853
Hard γ	17 Aug	17 Aug	E	-	-	0.6	390	375
Single lepton	17 Aug	18 Aug	μ	1	OV,1	1.4	362	116
Di-lepton	18 Aug	18 Aug	Eμ	2	OV,2	0.4	470	390
Di-lepton	18 Aug	22 Aug	Eμ	1	OV,2	1.0	1297	995
Single lepton	24 Aug	25 Aug	Eμ	1	OV,1	3.1	831	465

the data is not yet understood.

The left hand side of Fig. 8 shows the e^+e^-invariant mass spectrum from a preliminary analysis of a subsample of 2 million events of the electron-triggered di-lepton sample. The analysis defines tracks by matching calorimeter clusters with track segments in the vertex detector. To eliminate background, each electron candidate is required to have an associated bremsstrahlung cluster in the calorimeter from radiation in front of the magnet. The analysis yields a preliminary value for the J/ψ production cross section of 270 ± 128 nb/nucleon. The error is currently dominated by the simulation of calorimeter acceptance which was still evolving while the data was being accumulated in April and May. Analysis of the full sample is underway.

The right hand plot in Fig. 8 shows the $\mu^+\mu^-$ mass spectrum from $\approx 80\%$ of the di-muon sample. The peak is some 30 MeV lower than the accepted value of the J/ψ and has a width of 75 MeV, compared to a Monte Carlo value of 60 MeV. The total J/ψ sample of 3000 events is being used to tune vertex packages. The final goal of the analysis is to detect displaced vertices which can then be used to determine the $b\overline{b}$ cross section.

The left hand plot in Fig. 9 shows the distribution of the z difference between primary vertex and $\mu^+\mu^-$ vertex for selected $\mu^+\mu^-$ pairs in the J/ψ region. The right hand plot in Fig. 9 shows the same distribution but with the additional requirement that at least one extra track is consistent with having originated at the $\mu^+\mu^-$ vertex. Despite the low statistics, the plots demonstrate the capacity to reconstruct detached vertices. A $b\overline{b}$ cross section of 12 nbarn would contribute about two $\mu^+\mu^-$ pairs. We expect that ongoing optimization of software tools and alignment will further decrease the background on these plots in the near future.

It is evident that a measurement of the $b\overline{b}$ cross section can only come from an analysis of the full J/ψ sample collected with the electron trigger. We estimate that the sample contains about 30,000 reconstructible J/ψ's without bremsstrahlung cut, about 20 of which come from b decay. The bremsstrahlung cut would reduce this to 3000 J/ψ's, not enough for a cross section measurement. However, other combinations of cuts, including a secondary vertex cut may allow a signal to emerge. The analysis is in progress.

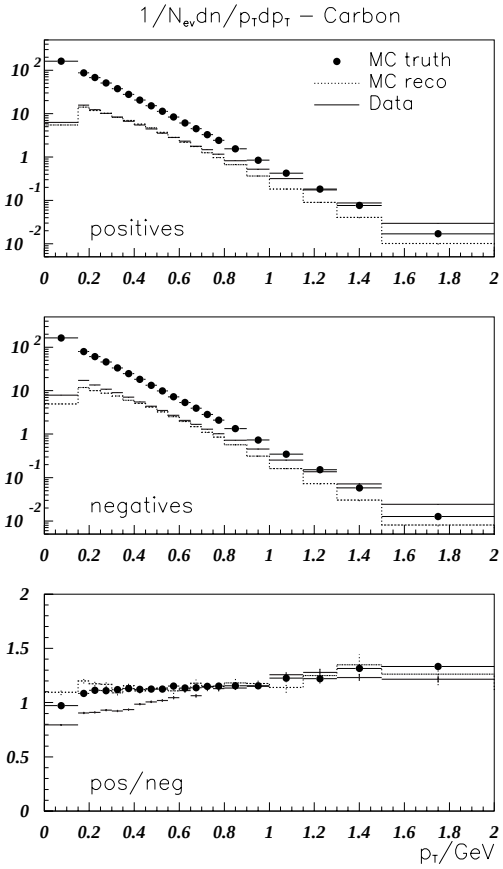

Figure 7: *Transverse momentum spectra for inelastic interactions in proton-carbon scattering. The data for positives and negatives are compared to Monte Carlo predictions after reconstruction and on the generator level ("truth"). Also shown is the ratio of positives to negatives.*

Finally, in Fig. 10, we show the $\pi^{\pm}K^{\mp}$ mass spectrum from the 1.2 million event sample collected with a single muon high-p_T ($p_T > 1.2$ GeV) trigger requirement run of Aug. 17. The $\pi^{\pm}K^{\mp}$ candidates were required to have a vertex separation of at least 2 mm. The candidates were required to have a RICH identification consistent with a pion hypothesis and the kaon candidates were required to be both consistent with a kaon hypothesis and inconsistent with a pion hypothesis. A D^0 signal is also seen in all of the hard-triggered (single lepton and di-lepton) data samples.

1.5 Physics Prospects

The chapter entitled "HERA – B Physics Beyond the Shutdown" is a compilation of 16 contributions by 20 authors. Each section evaluates the HERA – B potential to contribute to particular physics topics. The topics fall into 3 main categories: B physics, charm physics and QCD studies. The level of simulation ranges from the generator level through to complete detector simulation and reconstruction using the standard reconstruction software.

We have chosen to delve into three topics in the field of B physics in more detail in this summary:

- CP Violation in $B^0 \to J/\psi\, K^0_S$ Decays: It now appears unlikely that HERA – B will contribute

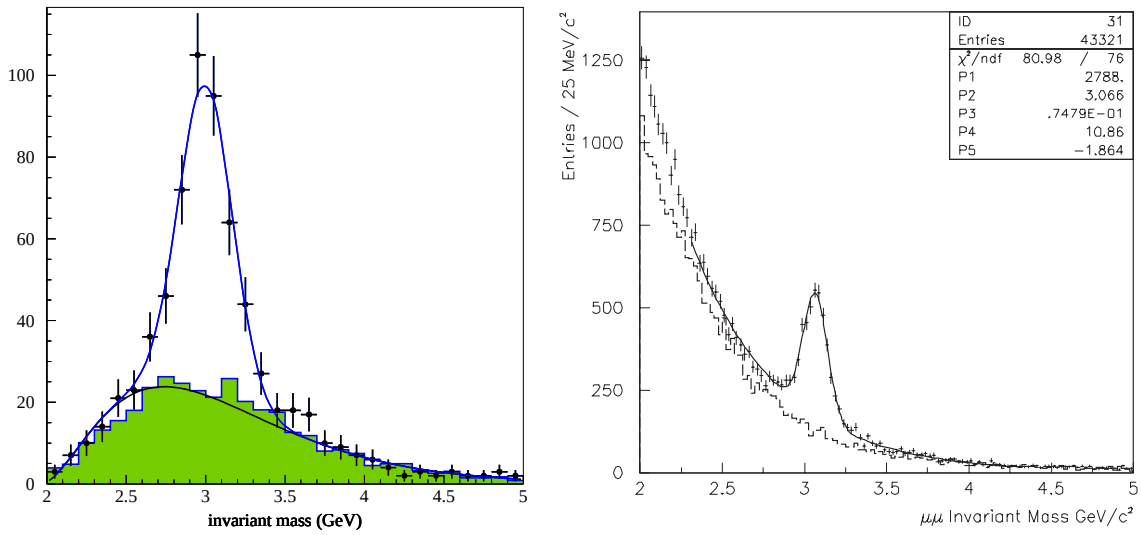

Figure 8: *The left hand plot shows the* e^+e^- *invariant mass spectrum from 10% of the electron-triggered data. The right hand plot shows the* $\mu^+\mu^-$ *and* $\mu^\pm\mu^\pm$ *(histogram) invariant mass spectra from 80% of the muon triggered data.*

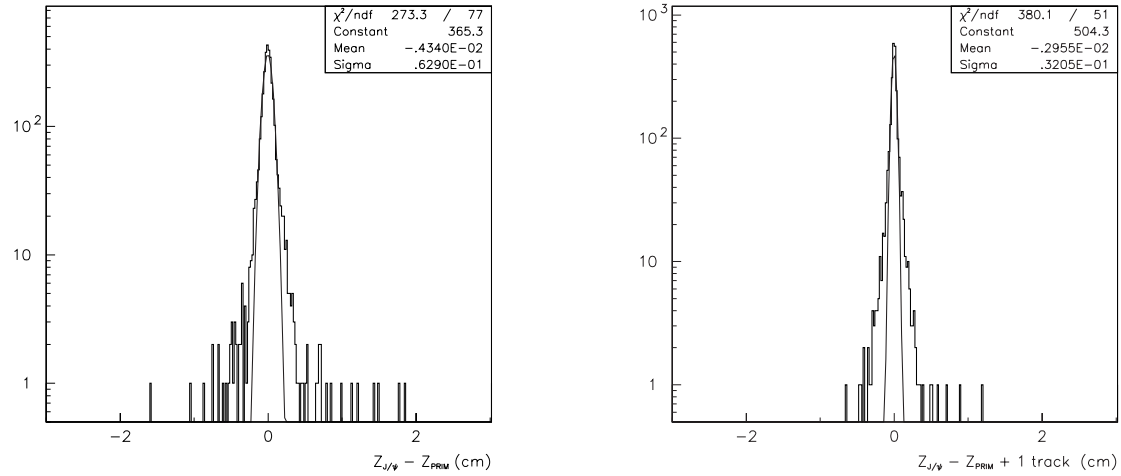

Figure 9: *The left hand plot shows the distribution of the z difference between primary vertex and* $\mu^+\mu^-$ *vertex for selected* $\mu^+\mu^-$ *pairs in the J/*ψ *region. The right hand plot shows the same distribution but with the additional requirement that at least one extra track is consistent with having originated at the* $\mu^+\mu^-$ *vertex.*

to this measurement at a level comparable to the e^+e^-experiments. Nonetheless, a significant measurement is still possible. Furthermore, a new visit to this topic gives the opportunity to update sensitivity estimates made at the time of the proposal in the light of a much more detailed simulation and full reconstruction.

- The flavor changing neutral current decay: $B^0 \to \mu^+\mu^- K^{*0}$. The Standard Model offers testable predictions for the decay rate of this process which is highly sensitive to new physics, such as charged Higgs bosons or heavy supersymmetric particles. HERA – B has the potential to compete

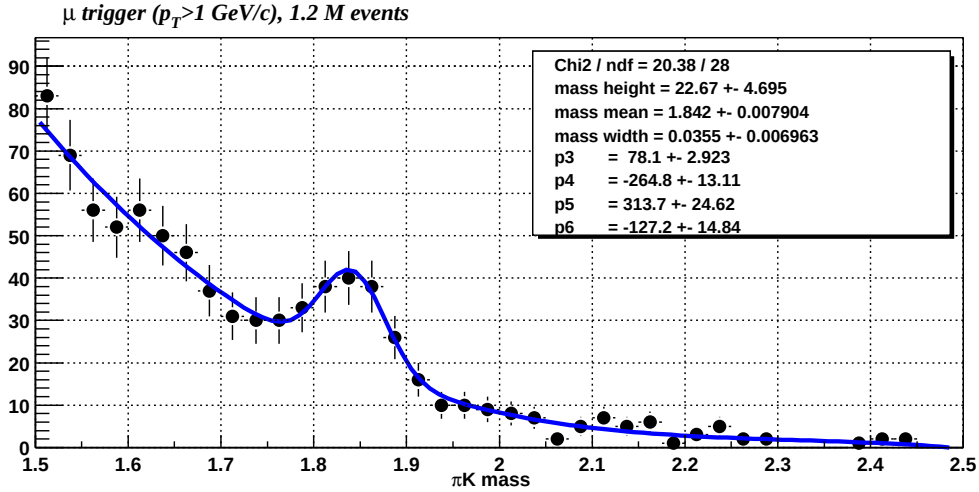

Figure 10: *Invariant mass spectrum of $\pi^{\pm}K^{\mp}$ candidates from a run taken with a trigger requiring a single high-p_T muon with $p_T > 1.2$ GeV.*

in this field with both e^+e^-machines and the TEV II experiments. $B^0 \to \mu^+\mu^- K^{*0}$ is but one of several exclusive final states relevant for FCNC studies.

- $B_s^0 - \overline{B_s^0}$ Mixing: This very challenging measurement can provide important constraints on parameters of the CKM matrix.

Before turning to these topics, we first comment in general on HERA – B potential for the topics studied. For most of the B physics measurements considered here, our most serious potential competition comes from the Tevatron RUN II program, depending on how quickly the Tevatron and the collider experiments reach design performance. Since we are unable to judge this, we offer two evaluations. The first, in Table 6, compares HERA – B's physics reach to existing measurements and extrapolations of existing experiments. The second, in Table 7 assumes that the TEV II experiments quickly reach design performance. Most likely, the situation by mid-2002 will be somewhere in between the scenarios.

In both tables, we indicate competitiveness for a baseline scenario which assumes a 20 MHz interaction rate, a single-track reconstruction efficiency of 80%, full trigger functionality and a $b\overline{b}$ cross section of 12 nb. We also indicate what would happen if the rate of accepted $b\overline{b}$ events falls below the baseline by a factor of 10. Once again, reality will most likely lie between these limits.

In the scenario of Table 6, it can be seen that, even for relatively modest assumptions on the performance of HERA – B, much of the field of heavy flavor physics is open to us. Even with optimistic assumptions on the capabilities of competing experiments, Table 7 shows that HERA – B can produce competitive or at least interesting and significant results in some areas of heavy flavor physics, but only if the baseline scenario is reached.

The interesting topics in the field of charm physics require a relaxation of trigger thresholds (invariant masses, transverse momenta etc.) and therefore greater demands are placed on the second and higher trigger levels. The feasibility is yet to be evaluated. Most likely a charm physics program can not be carried out in parallel with a B physics program in a transparent way.

It is noteworthy that the very preliminary study of measuring CP violation in $B^0 \to \pi^+\pi^-$ decays in this report shows promise. Assuming the branching fraction recently measured by the BABAR

Table 6: *Summary of requirements and performances of HERA – B for the main physics topics, measured against the presently available experimental results and extrapolations of existing experiments (excluding the TEV II experiments). Needed triggers are indicated by a cross. A double-cross indicates that the trigger must be operated at reduced thresholds (invariant masses, transverse momenta etc.). The assessment of competitiveness is made for a baseline scenario which assumes an interaction rate of* 20 MHz*, a conservative single-track reconstruction efficiency of* 80%*, and the full trigger functionality. A second scenario is included which assumes that the reconstructed* $b\overline{b}$ *rate is 10% of the baseline. The* $b\overline{b}$ *production cross section is assumed to be* 12 nb *per nucleon for the baseline scenario (more precisely, a* $b\overline{b}$ *production rate of* 18 Hz *is assumed), a value which is at the lower end of the range allowed by existing measurements. This cross section could be larger by up to a factor* 5*.*

Topic	Trigger Requirements μ	e	hpt	FLT	Competition	Potential (% of baseline) 100%	10%
B physics							
$\sigma_{b\overline{b}}$	×	×	–	×	-	***	***
$\sin(2\beta)$	×	×	–	×	e^+e^-,TEV I	*	–
$CP(B_s^0 \to J/\psi\Phi)$	×	×	–	×	LEP,SLC,TEV I	*	–
b lifetimes	×	×	–	×	LEP,SLC,TEV I	***	**
$\Delta\Gamma_s$	×	×	–	×	LEP,SLC,TEV I	***	*
$B_s^0 \to \mu^+\mu^-$	×	–	–	×	CLEO,TEV I	***	**
$B^0 \to K^{*0}\mu^+\mu^-$	×	–	–	×	e^+e^-,TEV I	***	**
$B^0 - \overline{B^0}$ Mixing	×	×	–	×	e^+e^-,TEV I	*	–
$B_s^0 - \overline{B_s^0}$ Mixing	×	×	×	×	LEP,SLC,TEV I	***	–
α, γ	×	×	×	×	e^+e^-	*** (?)	–
rare B → hadrons	×	×	×	×	e^+e^-,TEV I	*** (?)	–
Charm physics							
$D^0 - \overline{D^0}$ Mixing	×	–	–	××	e^+e^-	**	*
$D^0 \to \mu^+\mu^-$	×	–	–	××	E771,e^+e^-	***	**
$D^0 \to e\mu$	×	(×)	–	××	E789,e^+e^-	***	**
QCD physics							
Drell-Yan	×	×	–	×	E866	***	**
Quarkonia	×	×	–	×	E866	***	**
soft pN	–	–	–	–	-	***	***
hard pN	–	×	(×)	(×)	-	***	***

*** Possible to perform the first or best measurement.
** Sensitivity worse than extrapolated values of competition but still interesting.
* Sensitivity comparable to existing measurements attainable.

experiment and that the FLT is operational with an overall trigger efficiency of 0.6, we obtain a surprisingly favorable result. Obviously this would be an important measurement and we are now investigating this possibility more carefully with a full simulation of the detector performance. It is worth noting that this measurement depends critically on K - π separation, as $B^0 \to \pi^+\pi^-$ decays must be distinguished from more copious $B^0 \to K^+\pi^-$. Such K - π separation is expected to be substantially better at HERA-B than at, e.g., CDF.

Table 7: *Assessment of the HERA – B physics potential as in Tab. 6, however measured against the full design performance of present and future competition, including the TEV II program.*

	Trigger Requirements				Competition	Potential (% of baseline)	
Topic	μ	e	hpt	FLT		100%	10%
B physics							
$\sigma_{b\overline{b}}$	×	×	–	×	-	***	***
$\sin(2\beta)$	×	×	–	×	e^+e^-,TEV II	*	–
$CP(B_s^0 \to J/\psi\Phi)$	×	×	–	×	TEVII	*	–
b lifetimes	×	×	–	×	TEVII	**	*
$\Delta\Gamma_s$	×	×	–	×	TEVII	**	–
$B_s^0 \to \mu^+\mu^-$	×	–	–	×	TEVII	**	–
$B^0 \to K^{*0}\mu^+\mu^-$	×	–	–	×	e^+e^-,TEV II	***	–
$B^0 - \overline{B^0}$ Mixing	×	×	–	×	e^+e^-,TEV II	*	–
$B_s^0 - \overline{B_s^0}$ Mixing	×	×	×	×	TEVII	**	–
α, γ	×	×	×	×	e^+e^-,TEV II	** (?)	–
rare B → hadrons	×	×	×	×	e^+e^-,TEV II	** (?)	–
Charm physics							
$D^0 - \overline{D^0}$ Mixing	×	–	–	××	e^+e^-	**	*
$D^0 \to \mu^+\mu^-$	×	–	–	××	E771,e^+e^-	***	**
$D^0 \to e\mu$	×	(×)	–	××	E789,e^+e^-	***	**
QCD physics							
Drell-Yan	×	×	–	×	E866	***	**
Quarkonia	×	×	–	×	E866	***	**
soft pN	–	–	–	–	-	***	***
hard pN	–	×	(×)	(×)	-	***	***

*** Possible to perform the first or best measurement.
** Sensitivity worse than extrapolated values of competition but still interesting.
* Sensitivity comparable to existing measurements attainable.

For completeness, we note that HERA – B can make significant contributions in the areas of heavy quarkonium production and spectroscopy, and of the physics of soft and hard proton-nucleus interactions even in the most pessimistic scenario.

1.5.1 CP Violation in $B^0 \to J/\psi\ K_S^0$ Decays

The HERA – B detector was designed to reconstruct the final states $\mu^+\mu^-\,\pi^+\pi^-$ and $e^+e^-\,\pi^+\pi^-$ of the golden decay mode $B^0 \to J/\psi\ K_S^0$. At the time of the Design Report [1] many idealistic assumptions had to be made to estimate the reconstruction efficiencies for these decay modes. Since then software became available for track reconstruction and trigger simulation. Several studies have been performed using these programs [2, 3, 4]. The numbers presented here are based on the most recent ones [5].

Tab. 8 lists the current estimates of the reconstruction efficiencies for the muon and the electron channel in comparison to the Design Report. The L1 trigger efficiencies are the upper limit efficiencies

given in Tables 2 and 4. The reconstruction efficiencies are smaller now for various reasons. The actual mechanical constraints in the fabrication of the Outer Tracker and the compensation coil of the electron beam pipe lead to holes in the acceptance and to an increase in multiple scattering. The lifetime cut was increased in ref. [5] to improve background suppression. This reduces the efficiency by 18% but has practically no impact on the measurement error of $\sin(2\beta)$ since the CP asymmetry only builds up during the mean lifetime of the B meson and can hence anyway not be measured at very small decay times. The geometrical acceptance for pions from K^0_S decays is smaller due to fewer Inner and Outer Tracker super-layers in the magnet.

Table 8: *Reconstruction efficiencies for the golden decay mode in comparison to the Design Report. The K^0_S reconstruction in ref. [5] is too small due to a bug in the Monte Carlo simulation which was found recently [6]. The number listed here is the corrected one.*

	$B^0 \to J/\psi\, K^0_S \to \mu^+\mu^-\, \pi^+\pi^-$		$B^0 \to J/\psi\, K^0_S \to e^+e^-\, \pi^+\pi^-$	
	Design	ref. [5]	Design	ref. [5]
L1 trigger efficiency*	62%	49%	45%	30%
lepton tracking in PC	89%	87%	89%	87%
J/ψ vertex+mass	99%	91%	99%	92%
pion tracks (geometry, reconstr.)	63%	50%	63%	55%
K^0_S vertex+mass	97%	93%	97%	93%
B^0 vertex+mass	94%	88%	73%	56%
main vertex	-	92%	-	87%
vertex detector tracking	-	90%	-	90%
lepton particle ID	94%	94%	85%	85%
decay kinematics	80%	-	80%	-
lifetime cut	69%	57%	69%	71%
total	16%	7.1%	8.3%	3.3%

* The numbers in columns 3 and 5 are the upper efficiency bounds from Tables 2 and 4.

For the measurement of CP violation the flavor of the B meson at production time has to be determined (tagged). Several tagging methods have been developed by other experiments and their applicability in HERA – B has been studied repeatedly [4, 7, 8].

Every method has a certain efficiency ϵ for finding a tag and a probability χ of correctly measuring the b quark charge. Hence the measured asymmetry is smaller by the dilution factor $D = 2\chi - 1$ and the error on $\sin(2\beta)$ scales with the tagging power $P = D\sqrt{\epsilon}$. All studies yield similar results of $P \simeq 0.3$.

The "same side tagging" method has successfully been used by CDF [9] and was a powerful tag in their analysis of the golden decay mode [10]. So far this method was not studied by HERA – B. Hence it is conceivable that the achievable tagging power can be increased.

Tab. 9 lists the expected statistical error on $\sin(2\beta)$ for one and four years of running (10^7 s per year) for different scenarios: for the nominal detector at an interaction rate of 20 MHz, and for a 20% reduced single track reconstruction efficiency. The assumed $b\overline{b}$ production cross section is 12 nb/nucleon. Note that this number is at the lower end of the expectations from measurements [11, 12] ranging from 8 nb/nucleon to about 60 nb/nucleon when scaled to 920 GeV/c proton beam energy.

In the worst case the achievable error on $\sin(2\beta)$ is 0.22 for four years of nominal running of

Table 9: *The CP reach of HERA – B , assuming a 20 MHz interaction rate and efficiencies as given in Table 8 (nominal) and when an additional factor of 0.80 per track is applied to the efficiency estimates given in Table 8.*

	nominal	80% tracking eff.
$b\bar{b}$/year	1.8×10^8	1.8×10^8
$B^0 + \overline{B^0}$	1.5×10^8	1.5×10^8
golden decays	74000	74000
produced $\mu^+\mu^- \pi^+\pi^-$ evts	3060	3060
produced $e^+e^- \pi^+\pi^-$ evts	3060	3060
reconstr. $\mu^+\mu^- \pi^+\pi^-$ evts	220	90
reconstr. $e^+e^- \pi^+\pi^-$ evts	100	40
backgr. fraction in $\mu^+\mu^-$ channel	0	0
backgr. fraction in e^+e^- channel	0.1	0.1
tagging power	0.3	.28
error on $\sin(2\beta)$ after 1 year	0.24	0.40
error on $\sin(2\beta)$ after 4 years	0.13	0.22

HERA – B. In comparison BABAR, Belle and CDF plan to achieve an error around 0.11 for one year [13, 14, 15]. Even though the situation is less favorable for HERA – B our result will still be valuable. The value of $\sin(2\beta)$ is a fundamental number of the SM and several measurements obtained with different experimental techniques are obligatory, especially if the current central values of CDF on one hand ($\sin(2\beta) = 0.79 \pm 0.44$ [10]) and preliminary results from BABAR ($\sin(2\beta) = 0.12 \pm 0.35$ [16]) and Belle ($\sin(2\beta) = 0.45 \pm 0.45$ [17]) on the other hand sustain with increased statistics. An additional measurement even with lower precision could become important.

It has to be realized, of course, that the above projections assume a First Level Trigger running near the upper limit of the range allowed by the present understanding of the trigger efficiency. Should the trigger performance stay much below design, HERA – B will not be able to make a significant measurement in this field.

1.5.2 The FCNC Decay $B^0 \to \mu^+\mu^- K^{*0}$

One of the dominant mechanisms in the $B^0 \to \mu^+\mu^- + X_s$ decay is a flavor changing neutral current (FCNC) penguin diagram with an intermediate top quark $b \to t \to s$, and a W-boson loop. Because of the heavy intermediate particles the process is very sensitive to the presence of new physics. From the theoretical point of view, a measurement of the fully inclusive non-resonant FCNC decay $B^0 \to \mu^+\mu^- + X_s$ represents an ideal testing ground for the standard model due to the absence of uncertainties from the hadronic final state.

The exclusive decay channel $B^0 \to \mu^+\mu^- K^{*0}$, chosen to characterize the HERA – B potential in searching for FCNC decays, is theoretically more difficult to treat but has a very clean experimental signature, giving powerful handles for background suppression. The decay has a large predicted branching fraction[5][18, 19]: $(2.0 \pm 0.7) \cdot 10^{-6}$) compared to $(5.7 \pm 0.7) \cdot 10^{-6}$ for $B^0 \to \mu^+\mu^- + X$.

[5]This more recent estimate of the branching fraction is somewhat larger than that ($1.5 \cdot 10^{-6}$) given later in this report. See also [20]

An important observable in this decay is the di-muon invariant mass spectrum or equivalently the differential decay rate as a function of s, the squared invariant mass of the di-muon system. The SM prediction, as well as the predictions for two other models, for the differential decay rate is shown in Fig. 11 (for details refer to [21]).

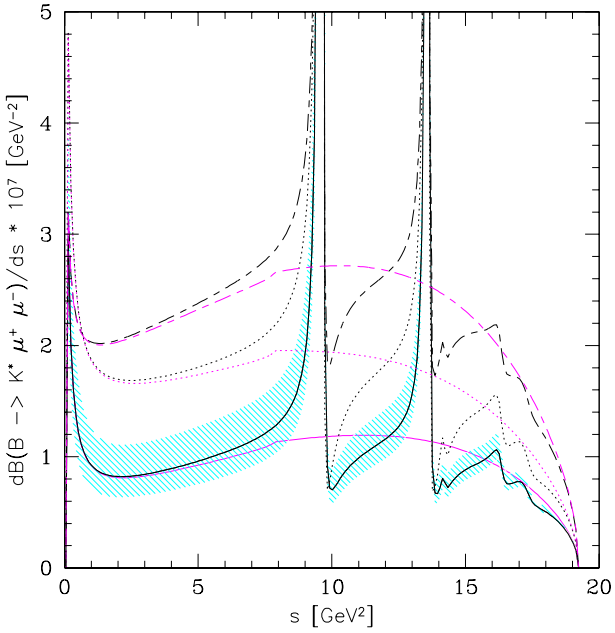

Figure 11: *The dilepton invariant mass distribution in* $B^0 \to \mu^+\mu^- K^{*0}$ *decays[21], using the form factors from LCSR as a function of s. The solid lines represents the SM and the shaded area depicts the form factor related uncertainties. The dotted lines corresponds to the SUGRA model. The long-short dashed lines correspond to an allowed point in the parameter space of the MIA-SUSY model. The corresponding pure SD spectra are shown as the lower curves in each case.*

Estimates for HERA – B acceptance and reconstruction efficiency for $B^0 \to \mu^+\mu^- K^{*0}$ are derived from an estimate of $B^0 \to J/\psi K^{*0}$ efficiency, based on a GEANT simulation and reconstruction using existing software packages. The trigger will be less efficient for $B^0 \to \mu^+\mu^- K^{*0}$ compared to $B^0 \to J/\psi K^{*0}$ because of p_T and mass cuts. Based on Fig. 11, we estimate that a 2 GeV mass cut will cut an additional 25% of the signal after p_T cuts.

The efficiency estimates are summarized in Tab. 10, assuming a (reduced) total interaction rate of 20 MHz and a conservative reconstruction efficiency of 80% per track. The First Level Trigger efficiency is the upper limit efficiency given in Table 4. Combining all factors, the total efficiency for detection and reconstruction of the FCNC decay $B^0 \to K^{*0}\mu^+\mu^- \to K^+\pi^-\mu^+\mu^-$ is about 6% corresponding to about 13 observed events per year. At the same time, roughly 1000 examples of the $B^0 \to J/\psi K^{*0}$ would be collected.

The decay $B^0 \to K^{*0}\mu^+\mu^-$ has been studied extensively by the BABAR collaboration (cf. [22] and references therein). BABAR expects a final statistics of 8 events[23] in a full year run with a nominal integrated luminosity of $30\,\mathrm{fb}^{-1}$. The CDF collaboration quotes a similar sensitivity, down to a branching fraction of 2×10^{-7} (corresponding to roughly 10 events) with the expected integrated luminosity of $2\,\mathrm{fb}^{-1}$ for Tevatron RUN II [24]. To gain enough statistics to measure the mass spectrum and a predicted forward-backward asymmetry in the $\mu^+\mu^-$system[18, 19], however, an integrated luminosity of $\mathcal{O}(10\ \mathrm{fb}^{-1})$ would be needed [25]. Any potential of HERA – B to measure

Table 10: *Estimate of HERA – B sensitivity for the non-resonant FCNC decay* $B^0 \to K^{*0}\mu^+\mu^- \to K^+\pi^-\mu^+\mu^-$ *for one year of running at a (reduced) interaction rate of* 20 MHz *and an assumed conservative single track reconstruction efficiency of* 80%. *The total trigger efficiency is denoted by* ϵ_{trig}.

Production per Year:	
$b\overline{b}$ per year	1.8×10^8
$B^0 + \overline{B^0}$ per year	1.5×10^8
$B^0 \to K^{*0}\mu^+\mu^- \to K^+\pi^-\mu^+\mu^-$	210
Acquisition and Reconstruction:	
FLT efficiency (incl. Geo, p,p_T cuts, tracking)(Table 4)	49%
FLT mass cut	75%
reconstruction efficiency $\mu^+\mu^-$	64%
geometrical acceptance $K^{*0} \to K^+\pi^-$	84%
reconstruction efficiency $K^{*0} \to K^+\pi^-$	64%
Background Cleaning:	
Jψ, ψ' mass cuts ($\pm$ 150 MeV)	75%
decay vertex cut ($\Delta z > 5$ mm)	62%
total efficiency	0.06
$B^0 \to K^{*0}\mu^+\mu^- \to K^+\pi^-\mu^+\mu^-$ per year	12.6

this FCNC process is therefore important in order to increase the world statistics necessary for sensitive tests of the standard model.

In conclusion, HERA – B has a chance to contribute in a significant way to the world statistics expected for the next years, provided that the di-muon trigger is running close to the upper limit of the range given in Table 4. So far, study of the HERA – B capability to measure this decay mode has been limited to efficiency estimates. An in depth analysis of possible background sources is beginning. HERA – B's excellent vertex detection and particle identification capabilities are powerful tools for background suppression which may also allow study of the inclusive process $B^0 \to \mu^+\mu^- + X_s$. It is perhaps also worth pointing out that many of the final states in the "X_s" system will also be reconstructible, such as $B^0 \to K^{*0}\pi^+\pi^-\mu^+\mu^-$, as well as decays of the charged B mesons: $B^+ \to K^+\,\pi^+\,\pi^-\,\mu^+\mu^-$. Channels such as $B^0 \to K^{*0}\,\pi^0\,\mu^+\mu^-$ may also be accessible.

1.5.3 B_s^0–$\overline{B_s^0}$ Mixing

The measurement of the B_s^0 oscillation frequency, Δm_s, provides important constraints on parameters described by the unitarity triangle. Present lower limits on Δm_s are set by LEP experiments, SLD and CDF, all using semi-leptonic B_s^0 decays. Because of the missing neutrino, the proper time resolution for B_s^0 decays in these experiments is not sufficient to discern the very rapid oscillations that are expected. To improve the Δm_s reach, one needs fully reconstructed B_s^0 decays. Among the most promising decay modes are $B_s^0 \to D_s^-\pi^+$ and $B_s^0 \to D_s^-\pi^+\pi^+\pi^-$. These final states have relatively large branching ratios and low multiplicities. The CDF group realized the importance of these decays and is constructing a special all-hadronic trigger for RUN II in order to accept them. These decays can also be detected at HERA – B.

B_s^0 decays to $D_s^-\pi^+$ and $D_s^-\pi^+\pi^+\pi^-$ can be accepted by a hadron-lepton trigger [1]. The requirements we consider at the first-level of the HERA – B trigger are a high-p_T charged track

($p_T > 1.5$ GeV/c) and a high-p_T lepton ($p_T > 1.0$ GeV/c for muons and $p_T > 1.4$ GeV/c for electrons). The high-p_T lepton is produced in the semi-leptonic decay of the second B hadron present in the event. The charge of the lepton track provides a high quality tag.

Using data taken in the year 2000 run and Monte Carlo, we estimate a combined suppression from pretriggers and FLT of 3000 for electron/high-p_T triggers and 290 for muon/high-p_T triggers, corresponding in an SLT input rate of 35 kHz. This is somewhat lower than the SLT design input rate of 50 kHz. The SLT suppression from tracking, an impact parameter cut on the pion and lepton identification is estimated to be a factor of 100. This leads to an output rate of 350 Hz. At the third level, the presence of a second B meson in the event can be used to further suppress background. This is under study.

As shown in Table 11, we plan to reconstruct B_s^0 mesons in 9 decay modes, most of which were reconstructed by LEP experiments. We expect that the excellent vertex resolution and kaon identification at HERA – B will allow sufficient suppression of combinatorial background also in high multiplicity modes.

The result of efficiency studies are summarized in Table 11. The high-p_T pretrigger efficiency was estimated using a full Monte Carlo simulation. The efficiencies of the muon and ECAL pretriggers as well as the FLT are provisionally assumed to be 1 (more below). SLT efficiencies are based on currently achieved values. The reconstruction efficiency is based on performance studies of the tracking algorithms for 1 + 4 interactions. In addition, the 17% of tracks which interact in the material of the spectrometer are assumed to be lost. The number of events reconstructed with this standard technique are listed in Table 11.

The efficiency can be improved considerably if one starts reconstruction in the vertex detector and does not require that the track passes the full tracking system. Moreover, if the track direction is determined in the vertex detector, its momentum can be obtained from kinematical constraints. Such a procedure does not deteriorate the proper time resolution significantly. The numbers of events reconstructed with this method are shown in Tab. 11.

The tagging power is larger than the P $\approx .3$ (see Sec. 1.5.1) derived in other HERA – B studies because the triggering lepton is used for a tag. The tagging efficiency is therefore 1 and the high-p_T lepton requirement assures a high quality. We estimate a tagging power P ≈ 0.6.

Two background sources were studied: inelastic events where the tagging lepton is fake and both reconstructed D_s^- and B_s^0 are fake, and $c\overline{c}$ events where the tagging lepton is real while the reconstructed D_s^- meson is either real or fake and the reconstructed B_s^0 meson is fake. The estimated signal-to-background ratio (S/B) from these sources is about 20.

The B_s^0 proper time resolution is dominated by vertex resolution which we estimate at $\sigma_z = 356\,\mu$m for the $D_s^-\pi^+$ and $\sigma_z = 338\,\mu$m for $D_s^-\pi^+\pi^+\pi^-$. Using the target wire constraint, the primary vertex resolution is 150 μm. The resulting proper time resolution is $\sigma_t = 0.060$ ps and $\sigma_t = 0.057$ ps for the $D_s^-\pi^+$ and the $D_s^-\pi^+\pi^+\pi^-$ decay modes, respectively.

In addition to the events listed in Table 11, we expect to collect 56 (22) reconstructed $B_s^0 \to D_s^{*-}\pi^+(\pi^+\pi^-)$ decays in the same period of time. The B_s^0 invariant mass distribution for the D_s^{*-} modes with a missing photon is estimated to be five times wider than that for the fully reconstructed D_s^- modes and the background is expected to be correspondingly larger, but still we expect a large signal-to-background ratio. In addition we expect to collect 34 (20) $B_s^0 \to D_s^{*-}\pi^+(\pi^+\pi^-)$ decays with kinematically determined momentum of one of the tracks reconstructed in the VDS only.

Fig. 12 shows the expected significance of our measurement of B_s^0 oscillations, using both the

Table 11: *Expected fraction of signal events per inelastic (minimum bias) event.*

	$B_s^0 \to D_s^- \pi^+$	$B_s^0 \to D_s^- \pi^+ \pi^+ \pi^-$
Physics:		
$\sigma_{b\bar{b}}/\sigma_{inel.}$	10^{-6}	10^{-6}
$b\bar{b} \to B_s^0$ (or $\overline{B_s^0}$)	0.16	0.16
$B_s^0 \to D_s^- \pi^+ (\pi^+ \pi^-)$	3.0×10^{-3}	8.0×10^{-3}
$D_s^+ \to \phi\pi^+ \to K^+K^-\pi^+$	0.018	0.018
$K^+\overline{K^{*0}} \to K^+K^-\pi^+$	0.022	0.022
$(K^+K^-\pi^+)_{nonres.}$	0.009	—
$K^+\pi^-\pi^+$	0.010	—
$\pi^+\pi^+\pi^-$	0.010	—
$K^{*+}\overline{K^{*0}} \to K_S^0\pi^+K^-\pi^+$	0.009	—
$\phi\pi^+\pi^+\pi^- \to K^+K^-\pi^+\pi^+\pi^-$	0.006	—
Total D_s^+ branching fraction	0.084	0.040
Trigger:		
Geometry, $p_T(\mu) > 1.0$ or $p_T(e) > 1.4\,GeV/c$	0.095	0.095
Pretrigger, $p_T(had) > 1.5\,GeV/c$	0.70	0.38
μ Pretrigger	1.0	1.0
e Pretrigger	1.0	1.0
FLT	1.0	1.0
SLT Slicer/Refit	0.9	0.9
Lepton ID	0.95	0.95
Geometrical acceptance	0.68	0.51
Track reconstruction (0.965×0.83 per track)	0.41	0.30
Main vertex	0.94	0.94
B_s^0 and D_s^- vertices	0.81	0.81
$VX(B_s^0) > 3.0\,mm$	0.66	0.66
$VX(D_s^-) > 4.5\,mm$	0.95	0.95
Summary	3.0×10^{-13}	1.1×10^{-13}
$B_s^0 \to D_s^- \pi^+ (\pi^+ \pi^-)$:		
#events/year	61	23
#events/year, 1 track reconstr. in VDS only	37	21
$B_s^0 \to D_s^{*-} \pi^+ (\pi^+ \pi^-)$:		
#events/year	56	22
#events/year, 1 track reconstr. in VDS only	34	20
Total number of events	188	86

$D_s^{(*)-}\pi^+$ and the $D_s^{(*)-}\pi^+\pi^+\pi^-$ decay modes modes, as a function of the oscillation parameter $x_s = \Delta m_s \cdot \Gamma_s$. Using the fully reconstructed $B_s^0 \to D_s^{(*)-}\pi^+(\pi^+\pi^-)$ decays, x_s values up to 24 can be measured at a $3\,\sigma$ level within one year of operation at 20 MHz interaction rate. We expect that we will find handles against the larger backgrounds[20] in the partially reconstructed decays. This would allow HERA – B to cover the complete range allowed by the Standard Model, assuming full pretrigger and FLT performance.

This conclusion is not significantly modified when the upper-limit trigger and pretrigger efficiencies arrived at in Sect. 1.3 are taken into account. The upper-limit efficiency for triggering on a

single muon (electron) and tracking it with the FLT algorithm is 89% (91%). Track-finding of the pion from the high-p_T pretrigger contributes another factor of 96% for a total efficiency of 86%. The statistical significance scales as the square root of the number of events, implying a loss of significance of just 7%.

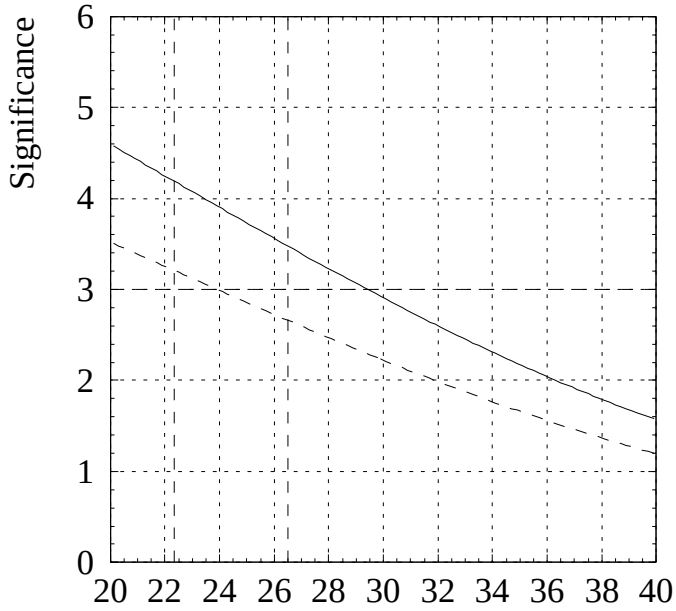

Figure 12: *Significance of* B_s^0 *oscillation measurements as function of* x_s*, expected to be achieved after one year of operation at an interaction rate of* 20 MHz*, using the* $D_s^{(*)-}\pi^+(\pi^+\pi^-)$ *decay modes (dashed line). The solid line shows the expected significance, if a kinematical reconstruction for the momentum of one of the tracks is also used. The present experimental lower limit and the upper limit from Standard Model fits are also indicated by vertical dashed lines.*

1.6 Conclusions

The HERA – B detector was completed in February of this year and has, for the most part, behaved stably. With some exceptions, the subsystems are either operating close to design or can be reasonably expected to approach design specifications with improvements already underway. Still, some work has yet to be finished and some concerns remain:

- The Outer Tracker was losing high-voltage channels at a high rate during the year 2000 run. The causes of this are believed to be understood and a remedy has been found. Investigations continue to determine if any of the observed failure modes are indicative of possible future problems.
- The efficiency of the muon system's pad chambers is low. Steps are being taken to improve it but full efficiency can probably only be reached if the preamplifiers are replaced. We are looking into the feasibility of doing so during the present shutdown.
- The optical links connecting chamber output to FLT are probably not sufficiently stable. A new link is being designed and the feasibility of replacing all or part of the system is under study.

- The readout electronics of outer chambers of the high-p_T system suffer from induced oscillations and noise pickup from an unknown source. This is not likely to be fatal since several similar systems have been made to work in the experimental hall but some additional experience with beam will most likely be necessary to fully debug the system.
- The capabilities of the FLT are not well known. Many tests have been performed but the results are not fully consistent. We expect that additional study of the data taken and of the simulation code will allow a clear picture to emerge on a time scale of several weeks. Until then, we cannot guarantee that the system will work close to design specifications.
- The ultimate rate capability of HERA – B is not yet known. The design calls for 40 MHz. To be more conservative, we have made the sensitivity estimates for this study assuming a 20 MHz interaction rate. It is not yet established that the trigger can operate without deadtime at even this rate.
- One item totally beyond our control but nonetheless relevant is the value of the $b\overline{b}$ cross section at 920 GeV which is still uncertain by nearly a factor of 8. (Our estimates assume a value of 12 nb, close to the low end (8 nb) of this range.

Many uncertainties remain but we have not found any fundamental flaw which would prevent HERA – B from working near to design.

The year 2000 run was used for commissioning the detector and triggering system. Data samples were accumulated with a combination of pretriggers and second level trigger. The data is under analysis and may be of sufficient quality to allow determination of the $b\overline{b}$ cross section. While the J/ψ signal in the $\mu^+\mu^-$mode is fairly clean, the signal can only be seen in the $e^+e^-$when inefficient particle id cuts are applied. We are looking into more efficient ways of reducing background (RICH cuts, improved E/p) but if none are found the utility of the e^+e^-decay mode for B studies will be limited.

Studies were performed to evaluate the potential of HERA – B to contribute to several areas of B-physics as well as charm-physics and QCD studies. The results are summarized in Tables 6 and 7. The general conclusion is that HERA – B can still be competitive in some areas such as a measurement of the $B^0 \to \mu^+\mu^-K^{*0}$ provided we succeed in operating close to design potential. Given the uncertainties listed above, this must be regarded as an "optimistic" scenario. In any case, there remains a good chance that HERA – B can provide meaningful and solid data in the area of B-physics, possibly charm physics and certainly QCD studies.

References

[1] E.Hartouni et al., HERA – B : Design Report, **DESY-PRC 95/01** (1995).

[2] M. Leuthold, *Untersuchung zur Effizienz der Rekonstruktion des Zerfalls* $B^0 \to J/\psi\, K^0_S$ *im HERA – B Experiment anhand vollständig simulierter Modellereignisse*, Diploma Thesis, Humboldt University, Berlin (1997).

[3] R. Mankel and A. Spiridonov, HERA – B internal notes 98-154 and 98-206, 99-111.

[4] M. Langer, *Bestimmung der Beauty-Quantenzahl bei HERA – B mit Hilfe Neutronaler Netze*, Diploma Thesis, Humboldt University, Berlin (1998).

[5] J. Ivarsson, *Potential for B-physics measurements with a fixed-target proton-collision experiment*, Ph.D. thesis, Lund University (1999); internal HERA – B note 99-105.

[6] J. Ivarsson, private communication.

[7] T. Lohse, HERA – B internal note 97-085.

[8] D. Samtleben, HERA – B internal note 98-080.

[9] F. Abe et al., Phys. Rev. **D59** (1999) 032001.

[10] T. Affolder et al., Phys. Rev. **D61** (2000) 072005.

[11] T. Alexopoulos et al.(E771), Phys. Rev. Lett. **82** (1999) 41, (hep-ex/9906022).

[12] D.M. Jansen et al.(E789), Phys. Rev. Lett. **74** (1995) 3118.

[13] The BABAR Physics Book, **SLAC-R-504** (1998). The error is 0.12/year.

[14] Belle Technical Design Report, KEK Report 95-1 (1995). The error is 0.11/year.

[15] The CDF-II Collaboration, Fermilab-Proposal-909 (1998). The error is 0.10/year

[16] D. Hitlin, ICHEP2000 conference in Osaka, Japan, preprint *hep-ex/0008048*.

[17] H. Aihara, ICHEP2000 conference in Osaka, Japan.

[18] A. Ali, Patricia Ball, L.T. Handoko and G. Hiller, Phys. Rev. D61 (2000) 074024. (hep-ph/9910221).

[19] A. Ali and G. Hiller, Phys. Rev. D60 (1999) 034017. (hep-ph/9807418).

[20] V. Egorytchev, V. Saveliev, P. Schlein, HERA-B 00-146 (4 October, 2000).

[21] G.Hiller, "$b \to s l^+ l^-$ decays in and beyond the Standard Model", SLAC-PUB-8851, Aug 2000.

[22] The BABAR Physics Book, *Physics at an Asymmetric B Factory*, eds. P.F. Harrison and H.R. Quinn, SLAC-R-504 (1998).

[23] F. Ferrarotto, F. Ferroni, M. Rotondo, BABAR note 432 (May 5, 1998).

[24] K.T. Pitts, *CP Violation, Mixing and Rare Decays at the Tevatron Now and in Run II*, Proc. 4th Conference on Heavy Quarks at Fixed Target, Batavia, IL, USA, 10 - 12 Oct 1998, AIP conf. proc. 459 (1998) 55-65.

[25] D.J. Jaffe, *Recent Results on Rare b Decays*, presented at 8th International Symposium on Heavy Flavor Physics (Heavy Flavors 8), Southampton, England, 25-29 Jul 1999, hep-ex/9910055.